Journal of Materials Science: Materials in Electronics
https://doi.org/10.1007/s10854-019-01902-z

Optimization on quality factor of $LaNbO_4$ microwave dielectric ceramics

Tian-Liang Tang[1] · Wang-Suo Xia[1] · Bo Zhang[1] · Ying Wang[1] · Ming-Xue Li[1] · Li-Wei Shi[1]

Received: 8 March 2019 / Accepted: 18 July 2019

Abstract
MgO was designed as a new additive to optimize the microwave dielectric properties of $LaNbO_4$ ceramics, and consequently the $Q\times f$ values of $LaNbO_4$ ceramics were effectively increased. The effects of MgO additive on phase composition, microstructure and microwave dielectric properties were discussed. $LaNbO_4$, indexed as the main phase, had no obvious change, while the secondary phase related to MgO varied with different MgO content. The grain growth was evaluated by grain size and its distribution. The dielectric constant (ε_r) was generally stable among the whole designed sintering temperature, but had some decrease with MgO (low permittivity) content increasing. The $Q\times f$ values were not only affected by bulk densities during the sintering process, but also depended on the grain size and its distribution with different MgO contents. Sintered at 1425 °C for 4 h with x = 0.5, $LaNbO_4$–xMgO ceramics possessed excellent performance: $\varepsilon_r = 19.8$, $Q\times f = 94{,}440$ GHz, $\tau_f = 6.1$ ppm/°C.

1 Introduction

Microwave dielectric ceramics, which played an important role in microwave communication system, were required to possess three characteristics: (1) appropriate dielectric constant, (2) ultra-low dielectric loss (high-quality factors), (3) a near-zero temperature coefficient of resonant frequency (τ_f) [1–3]. With the development of mobile communication, especially the arrival of 5G era, higher requirements were desired on microwave dielectric properties.

Rare-earth niobate system ($ReNbO_4$: Re = La, Nd, Sm, Dy, Er, Lu, Y, Yb and Ce) was a series of typical microwave dielectric ceramics with low permittivity and relatively high $Q\times f$ values, which had been widely reported [4, 5]. In previous reports, the microwave dielectric properties of Rare-earth niobate were εr = 12–26, $Q\times f$ = 33000–56600 GHz, which were good for microwave application in the past. However, under the new development requirements, the $Q\times f$ values of $ReNbO_4$ ceramics had no obvious advantage compared with other low-permittivity systems. Although many researches about the modification on $ReNbO_4$ ceramics had already been reported [6–19], the optimization effect of $Q\times f$ values was not obvious. Thus, optimizing the $Q\times f$ values of $ReNbO_4$ ceramics to adapt to the higher requirements was of great necessary, which was just the aim of this paper.

In this paper, $LaNbO_4$, a typical representative of $ReNbO_4$ ceramics, was chosen as the study subject, and MgO was selected as a new additive to optimize the $Q\times f$ values of $LaNbO_4$ ceramics. Expectedly, the optimization effect on the $Q\times f$ values was remarkable. Additionally, the influencing factors for microwave dielectric properties of $LaNbO_4$ ceramics with different MgO-addition content had also been investigated.

2 Experimental procedure

$LaNbO_4$–xMgO samples were prepared through a conventional sintering reaction process, and the raw materials, La_2O_3 (99.95%), MgO (99%) and Nb_2O_5 (99.99%), were weighed according to the stoichiometric amount of $LaNbO_4$–xMgO (x = 0.25, 0.5, 1.0, 2.0, 3.0, respectively). All weighed powders were orderly added to nylon cans and milled for 6 h with distilled water as dispersive media. After milling, the slurries were dried at 100 °C for 12 h.

✉ Wang-Suo Xia
xiaws@cumt.edu.cn

✉ Li-Wei Shi
liwei5450@cumt.edu.cn

[1] School of Physical Science and Technology, China University of Mining and Technology, Xuzhou 221116, China

Published online: 22 July 2019

Then the dried powders, which were crushed and screened, then calcined at 1100 °C for 4 h. Next, the mixture was reground for 24 h, then dried, crushed and sieved with 80 mesh screen. Finally, the powders were pressed into pellets (Ø10 mm × 5 mm) with 10 wt.% paraffin as the binder. These pellets were sintered at 1350–1475 °C for 4 h with the heating rate of 5 °C/min.

The bulk densities of the sintered pellets were measured using the Archimedes method. The microstructure on the ceramic surfaces was analyzed by a field emission scanning electron microscopy (FE-SEM, SIGMA Zeiss, Germany). The average grain size and its distribution of the prepared samples were analyzed from SEM images. The crystal structure and phase composition of the ceramics were investigated according to X-ray diffraction (XRD, Model D/Max-B, Rigaku Co., Japan). The phase composition and element distribution of pellets were confirmed by energy dispersive spectrometer (EDS). The ε_r and $Q \times f$ values of the synthesized pellets were collected through a network analyzer (E5063A, Keysight Co., USA) at the microwave frequency ranged from 8 to 14 GHz using $TE_{01\delta}$ shielded cavity method [20, 21]. The temperature coefficient of resonant frequency was analyzed at the temperature points of 25 °C and 85 °C in $TE_{01\delta}$ mode, which could count according to the following formula:

$$\tau_f = \frac{f_2 - f_1}{f_1(T_2 - T_1)} \quad (1)$$

where f_1 and f_2 were the resonant frequency at T_1 and T_2, respectively.

3 Results and discussion

Figure 1 showed the SEM images of $LaNbO_4$–xMgO (x = 0.25, 0.5, 1.0, 2.0, 3.0) samples at the optimum sintering temperature, from which the statistical distribution of grain size could be clearly seen. For each sample, the grain boundaries were straight with no pores being observed, indicating that the dense samples had been obtained, which was benefit to excellent microwave dielectric properties. Furthermore, it was important to noted that two kinds of crystalline grains were surrounded by each other, which could be clearly observed from Fig. 1b–e, implying that the samples might be composed of two phases. In addition, the average grain size (Agz) and its distribution (expressed by standard deviation abbreviated as SD) were calculated to evaluate the grain growth of $LaNbO_4$ ceramics with different MgO content. As shown in the inset of Fig. 1, the Agz and sd values both presented a decreasing tendency, which decreased from 1.60 to 0.81 μm, and 0.88 to 0.38 respectively, suggesting that MgO additive on one hand suppressed the grain growth of $LaNbO_4$ ceramics, but on the other hand was advantageous for grain size distribution.

The phase composition of $LaNbO_4$–xMgO (x = 0.25, 0.5, 1.0, 2.0, 3.0) ceramics was analyzed by the XRD, as shown in Fig. 2. Although, there were some differences in XRD patterns among each sample, as a whole two obvious phases, indexed as $LaNbO_4$ (Fergusonite structure, JCPDS no. 22-1125) and MgO (Cubic structure, JCPDS no. 45-0946), were detected in $LaNbO_4$–MgO ceramics. The certain differences among the XRD patterns of $LaNbO_4$–xMgO ceramics

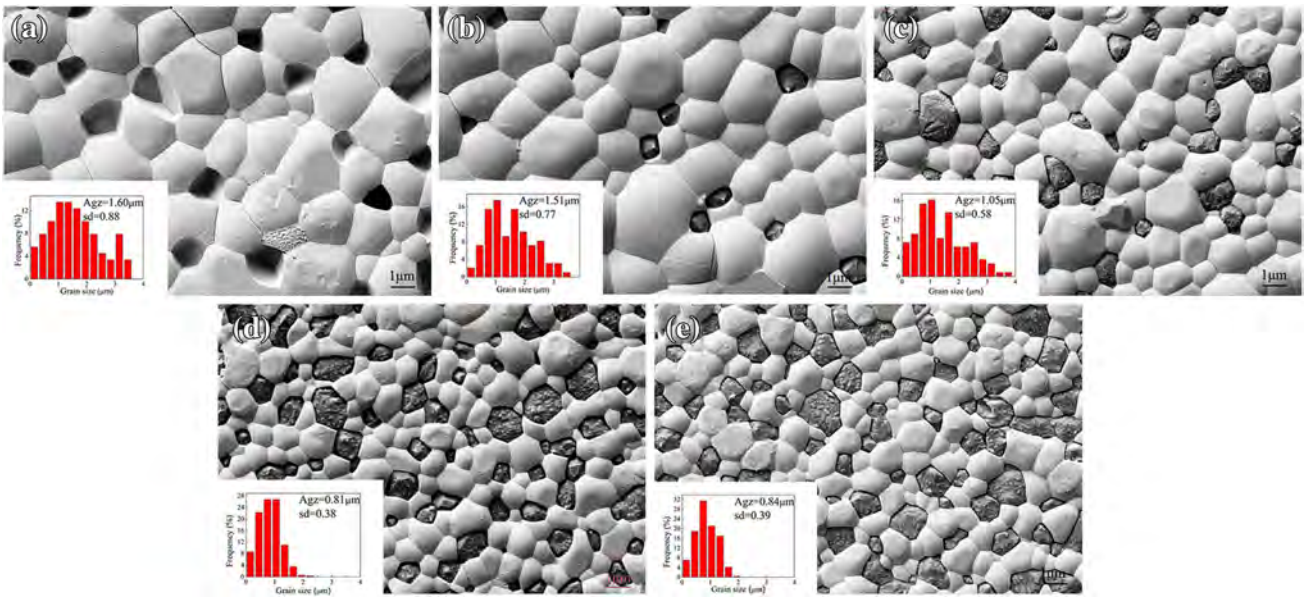

Fig. 1 The SEM images and statistical distribution for the grain size of $LaNbO_4$–xMgO (x = 0.25, 0.5, 1.0, 2.0, 3.0) ceramics

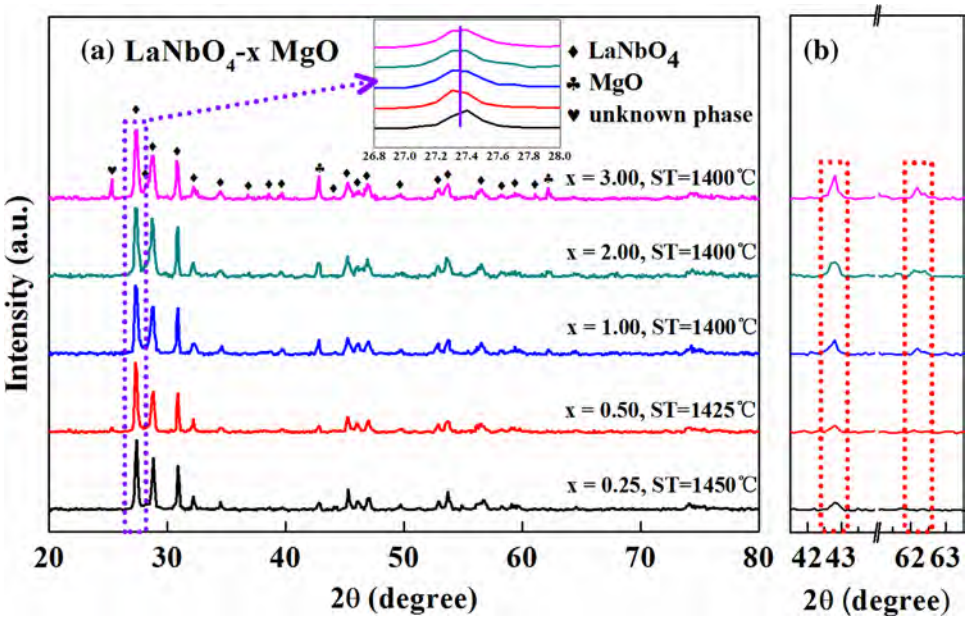

Fig. 2 The XRD patterns of $LaNbO_4$–xMgO (x = 0.25, 0.5, 1.0, 2.0, 3.0) ceramics

were appeared when x = 0.25 and x = 3.0. When x = 0.25, the XRD pattern presented pure phase indexed as $LaNbO_4$ owing to the amount of MgO content was too small to detect. When x = 3.0, there was an unknown phase observed (which would be discussed later in this article). For details from Fig. 2, the peak position of the two phases had no obvious shift with different MgO content. However, the relative peak intensity of MgO phase increased with the increasing MgO content, suggesting that $LaNbO_4$ phase and MgO phase were independent of each other and no chemical reaction occurred during the preparation processes. These results of XRD suggested that the $LaNbO_4$ phase was formed in the $LaNbO_4$–MgO ceramics, which did not change with different content of MgO additive.

In order to investigate the phase distribution and the unknown phase, the EDS had been utilized to study $LaNbO_4$–xMgO (x = 0.25, 0.5, 1.0, 2.0, 3.0) ceramics, with the results being illustrated in Fig. 3. Obviously, the La:Nb ratio of all samples was approximately 1:1 and the proportion of Mg element increased as the x value increase, indicating that the prepared samples were in accordance with our design, as shown in Fig. 3a. The distribution of each element was shown in Fig. 3b, taking x = 0.5 as an example. It could be noted that the distributions of La and Nb elements were the same as each other, and the distribution of Mg element was just complementary to them, which confirmed the fact that the $LaNbO_4$ phase and MgO phase was respectively formed and were surrounded by each other. Moreover, the element distribution when x = 3.0 (with an unknown phase appeared) was also detected, as shown in Fig. 3c. It was important to find that there was no significant difference in terms of type and distribution of sample elements appeared between the samples with x = 3.0 and x = 0.5, reflecting that the unknown phase appearing at x = 3.0 was related to relatively large amount of MgO additive. Obviously, the results of EDS analysis were strong proofs for SEM and XRD conclusions.

The dielectric constant and bulk densities of $LaNbO_4$–xMgO (x = 0.25, 0.5, 1.0, 2.0, 3.0) ceramics were shown in Fig. 4. Compared Fig. 4a with b, the curves of dielectric constant with different sintering temperature were similar to those of densities, owing to the reduction of pores during the densification process of ceramics. In addition, the changes of densities and dielectric constant were quite small during the sintering processes, indicating that the sintering temperature range of $LaNbO_4$–MgO ceramics was wide. Figure 4c showed the variation trend for dielectric constant of $LaNbO_4$–MgO ceramics as a function of MgO content. It was easy to find that the dielectric constant decreased as the increasing of MgO content. According to the previous structural analysis, phase composition was confirmed to be the main factor that led to the change in dielectric constant of $LaNbO_4$–MgO ceramics. For multiphase ceramics, the dielectric constant was satisfied with the Lichtenecker logarithmic superposition rule. Therefore, the dielectric constant of $LaNbO_4$–MgO ceramics exhibited the variation described above, on account of lower dielectric constant of MgO.

Figure 5 showed the $Q \times f$ values of $LaNbO_4$–xMgO (x = 0.25, 0.5, 1.0, 2.0, 3.0) ceramics with different sintering temperature and MgO content. As shown in Fig. 5a, the $Q \times f$ values of $LaNbO_4$–MgO ceramics increased to a maximum and then slightly decreased as a function of sintering temperature, which resulted from the changes in ceramic densification. The $Q \times f$ values of $LaNbO_4$–MgO ceramics with different MgO content were shown in Fig. 5b, which was the focus point of this paper. There

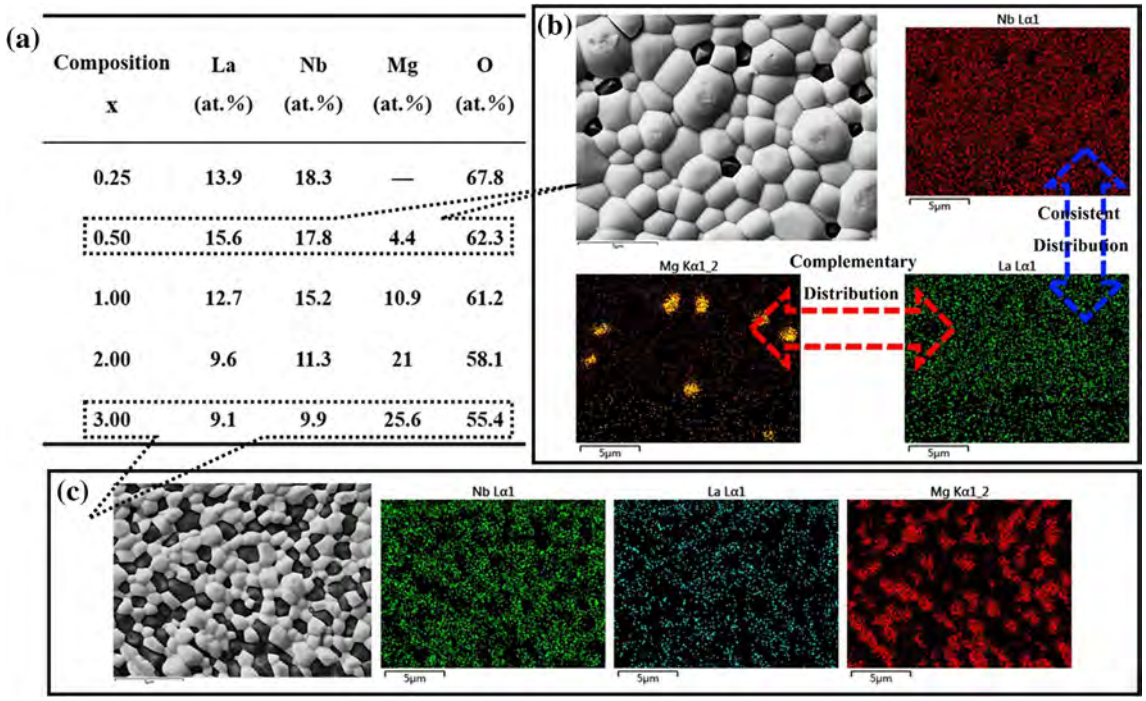

Fig. 3 The EDS images and the element distribution of $LaNbO_4$–xMgO (x = 0.25, 0.5, 1.0, 2.0, 3.0) ceramics

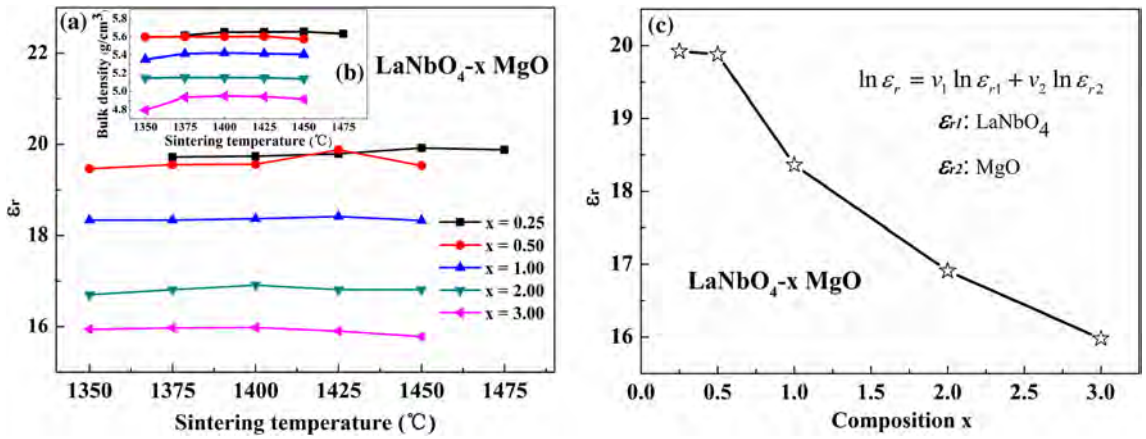

Fig. 4 The dielectric constant and the density of $LaNbO_4$–xMgO (x = 0.25, 0.5, 1.0, 2.0, 3.0) ceramics

were two key points in Fig. 5b, which were (1) the $Q \times f$ values of $LaNbO_4$ ceramics were significantly optimized, and (2) the $Q \times f$ values of the ceramics varied with MgO content. For the first point, there were two possible reasons, one was the high $Q \times f$ values of MgO, and the other was the matching of crystal structure between $LaNbO_4$ and MgO, which were two kinds of materials just within a similar c/a value (c/a ~ 1). For the second point, it was the competition results of grain size and the uniformity of grain size distribution. In other words, the $Q \times f$ values of $LaNbO_4$–MgO ceramics could be regulated by controlling the grain size and its distribution.

Figure 6 showed the temperature coefficient of resonant frequency of the $LaNbO_4$–MgO ceramics with different MgO content. Obviously, the curve of τ_f values presented a downward trend and was getting closer to zero with MgO content increasing. It was known that τ_f values were dependent on the additive and satisfied with the Lichtenecker logarithmic mixing rule. The τ_f values of the $LaNbO_4$–MgO ceramics shifted to the negative direction because MgO

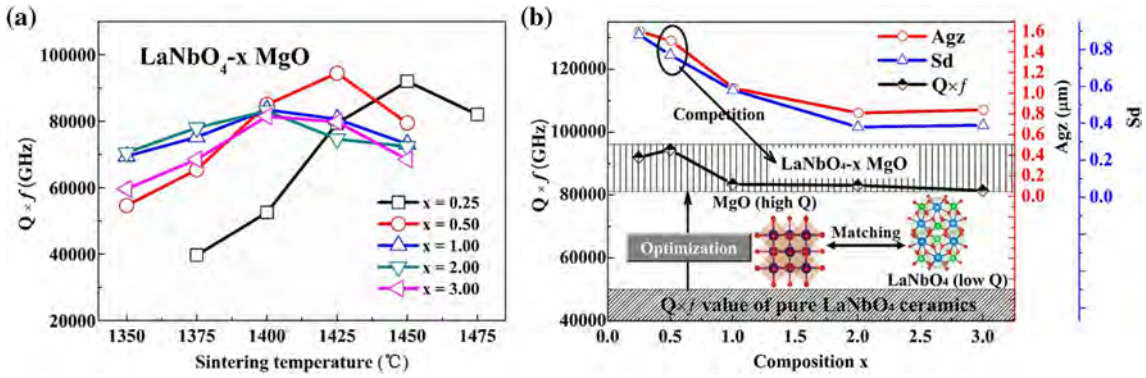

Fig. 5 The Q×f values of $LaNbO_4$–xMgO (x = 0.25, 0.5, 1.0, 2.0, 3.0) ceramics

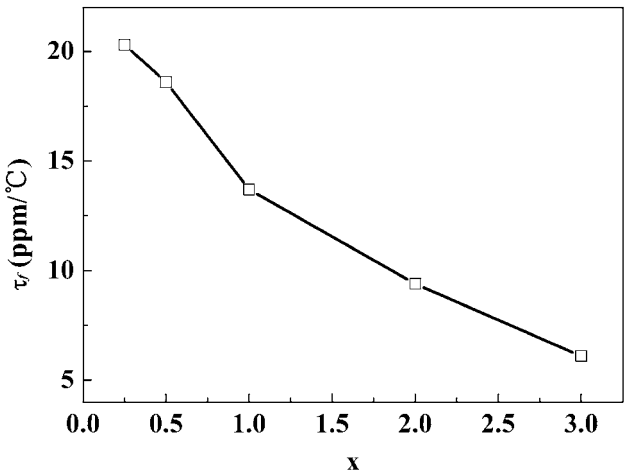

Fig. 6 The τ_f values of $LaNbO_4$–MgO ceramics with different MgO content

had a negative τ_f values. More importantly, the τ_f values of $LaNbO_4$ ceramics had no deteriorated with MgO additive, which was still a temperature-stable microwave dielectric ceramics.

4 Conclusion

Microwave dielectric properties of $LaNbO_4$ ceramics had been optimized effectively by MgO additive. The phase composition of $LaNbO_4$–MgO ceramics were generally two-phase coexistence, which indexed as $LaNbO_4$ and MgO. The distribution of the two phases was independent and surrounded with each other. The grain growth of $LaNbO_4$ ceramics was limited by MgO addition, but the uniformity of the grain size distribution was greatly optimized. The dielectric constants and Q×f values were related to bulk densities during the sintering process, which were explained by the densification of ceramics. When the MgO content changed, the change rule of the dielectric constant and τ_f values was satisfied with Lichtenecker logarithmic superposition rule. The Q×f values were depended on the competition results of grain size and grain uniformity. In addition, compared with pure $LaNbO_4$ ceramics, the Q×f values of $LaNbO_4$–MgO ceramics had been distinctly improved, probably because MgO had a high Q×f values and its crystal structure matched with $LaNbO_4$ phase. Consequently, MgO was an excellent additive in $LaNbO_4$ system for optimizing microwave dielectric properties.

Acknowledgements This work is supported by the National Natural Science Foundation of China under Grant No. 51702359 and the projects from the Fundamental Research Funds for the Central Universities of China University of Mining and Technology under Grant No. 2017XKQY016.

References

1. Y. Higuchi, H. Tamura, Recent progress on the dielectric properties of dielectric resonator materials with their applications from microwave to optical frequencies. J. Eur. Ceram. Soc. **23**, 2683–2688 (2003)
2. M.T. Sebastian, *Dielectric Materials for Wireless Communication* (Elsevier, Amsterdam, 2010)
3. R.J. Cava, Dielectric materials for applications in microwave communications. J. Mater. Chem. **11**, 54–62 (2001)
4. D.W. Kim, D.K. Kwon, S.H. Yoon, K.S. Hong, Microwave dielectric properties of rare-earth ortho-niobates with ferroelasticity. J. Am. Ceram. Soc. **89**, 3861–3864 (2006)
5. Z.L. Zhang, C. Xu, Q.P. Liu, Microwave dielectric properties of $ReNbO_4$ (Re = Y, Yb, Ce) ceramics. Key Eng. Mater. **434–435**, 217–220 (2010)
6. H.W. Lee, J.H. Park, S. Nahm, D.W. Kim, J.G. Park, Low-temperature sintering of temperature-stable $LaNbO_4$ microwave dielectric ceramics. Mater. Res. Bull. **45**, 21–24 (2010)
7. Y.H. Chen, H. Wang, L.X. Pang, H.F. Zhou, X. Yao, Effect of Zn^{2+} substitution on sintering behavior and dielectric properties of $NdNbO_4$ ceramics. Ferroelectrics **407**, 61–68 (2010)
8. P. Zhang, Z.K. Song, Y. Wang, Y.M. Han, H.L. Dong, L.X. Li, Effect of $CaTiO_3$ addition on microwave dielectric properties of

$NdNbO_4$ ceramics as multi-function material. J. Alloys Compd. **281**, 741–746 (2013)
9. Z.K. Song, P. Zhang, Y. Wang, L.X. Li, Improved quality factor of $NdNbO_4$ microwave dielectric ceramic by Mn^{2+} substitution. J. Alloys Compd. **583**, 546–549 (2014)
10. P. Zhang, Y.G. Zhao, New temperature stable $(Nd_{1-x}La_x)_{1.02}Nb_{0.988}O_4$ microwave dielectric ceramics. Mater. Lett. **161**, 620–623 (2015)
11. P. Zhang, Y.G. Zhao, H.T. Wu, X.Y. Wang, New temperature stable and low loss materials of $(Nd_{0.97}Mn_{0.045})_{1.02}Nb_{0.988}O_4$ ceramics by La^{3+} substitution. J. Alloys Compd. **650**, 547–552 (2015)
12. Y.G. Zhao, P. Zhang, Phase composition, crystal structure, complex chemical bond theory and microwave dielectric properties of high-Q materials in a $(Nd_{1-x}Y_x)NbO_4$ system. RSC Adv. **5**, 97746–97754 (2015)
13. P. Zhang, Y.G. Zhao, X.Y. Wang, The correlations between electronic polarizability, packing fraction, bond energy and microwave dielectric properties of $Nd(Nb_{1-x}Sb_x)O_4$ ceramics. J. Alloys Compd. **644**, 621–625 (2015)
14. P. Zhang, Y.G. Zhao, J. Liu, Z.K. Song, M. Xiao, X.Y. Wang, Correlation of crystal structure and microwave dielectric properties of $Nd_{1.02}(Nb_{1-x}Ta_x)_{0.988}O_4$ ceramic. Dalton Trans. **44**, 5053–5057 (2015)
15. S.D. Ramarao, V.R.K. Murthy, Structural phase transformation and microwave dielectric studies of $SmNb_{1-x}(Si_{1/2}Mo_{1/2})_xO_4$ compounds with fergusonite structure. Phys. Chem. Chem. Phys. **17**, 12623–12633 (2015)
16. P. Zhang, Y.G. Zhao, Influence of Sm^{3+} substitutions for Nd^{3+} on the microwave dielectric properties of $(Nd_{1-x}Sm_x)NbO_4$ (x = 0.02-0.15) ceramics. J. Alloys Compd. **654**, 240–245 (2016)
17. Y.G. Zhao, P. Zhang, Effects of lanthanides on structural and dielectric properties of $NdNbO_4$-$LnNbO_4$ ceramics. Ceram. Int. **44**, 1935–1941 (2018)
18. M. Xiao, Q.Q. Gu, Z.Q. Zhou, P. Zhang, Low temperature sintering behavior and microwave dielectric properties of $LaNbO_4$ ceramics with $BaCu(B_2O_5)$ additive. J. Alloys Compd. **730**, 528–532 (2018)
19. M. Xiao, Y.S. Wei, Q.Q. Gu, Z.Q. Zhou, P. Zhang, Relationships between bond ionicity, lattice energy, bond energy and the microwave dielectric properties of $La(Nb_{1-x}Ta_x)O_4$ (x = 0-0.1) ceramics. J. Alloys Compd. **775**, 168–174 (2019)
20. B.W. Hakki, P.D. Coleman, A dielectric resonator method of measuring inductive capacities in the millimeter range. IEEE Trans. Microw. Theory Tech. **8**, 402–410 (1960)
21. W.E. Courtney, Analysis and evaluation of a method of measuring the complex permittivity and permeability microwave insulators. IEEE Trans. Microw. Theory Tech. **18**, 476–485 (1970)